ORIGINAL ARTICLE



Bayesian monitoring of machining processes using non-intrusive sensing and on-machine comparator measurement

Moschos Papananias¹

Received: 1 October 2024 / Accepted: 3 February 2025 / Published online: 25 February 2025 © The Author(s) 2025

Abstract

Machining processes are largely reliant on manual intervention and non-value-added processes, such as post-process inspection, to achieve end-product conformance. However, the ever-increasing demand for high manufacturing productivity combined with low costs and high product quality requires online monitoring systems to provide real-time insights into the cutting process and minimize the volume of non-value-added processes. Most of the published work on machining process monitoring focuses on intrusive measurement equipment, such as dynamometers, to predict the dimensional quality of machined parts, preventing industrial exploitation due to practical limitations. The main focus of this work is to address this issue by developing a new product health monitoring method for machining processes using non-intrusive and low-cost instrumentation and data acquisition (DAQ) hardware. The sensing setup in this work includes an acoustic emission (AE) sensor and two accelerometers in the work holding. The proposed monitoring system is applied to milling experiments using Gaussian process regression (GPR) for probabilistic nonlinear in-process product condition monitoring. Validation results show the effectiveness of the GPR model to provide accurate probabilistic predictions of product health metric deviations with reasonable uncertainty estimates considering the large variability of the data. In addition, a Bayesian inference methodology is derived to dynamically incorporate subsequent information from on-machine probing (OMP) with a comparator method, improving the accuracy and robustness of the proposed solution. Specifically, it is demonstrated that a precision-weighted combination of prior information from the posterior predictive distribution for a future observation and new metrological information from on-machine comparator measurement (OMCM) can clearly improve posterior inferences about the end product condition.

 $\textbf{Keywords} \ \ \text{Bayesian inference} \cdot \text{Gaussian process regression} \cdot \text{Intelligent manufacturing} \cdot \text{Machining process monitoring} \cdot \text{On-machine comparator measurement}$

1 Introduction

Subtractive machining processes, such as turning, milling, drilling, and grinding, are highly complex manufacturing processes characterized by nonlinear dynamics involving many parameters and uncertainty sources. Therefore, the geometric deviation of machined parts from the design specifications is affected by a large range of interrelated influencing factors, which are difficult to estimate [1]. Such processes are generally planned by highly skilled manufacturing

engineers and machinists based on their knowledge and previous experience, theoretical modelling of the process, and specialized machining simulation software to achieve parts with precise dimensions and desired surface finish. However, many failure modes with high scrap levels are still observed in a production setting due to a variety of causes and errors typified by nonlinearities and time-varying characteristics. Under these circumstances, knowledge about the machining process is usually incomplete and prediction models must be able to cope with substantial uncertainty. The task of controlling such systems is a considerable challenge in many applications [2, 3].

Machining processes are typically followed by inspection processes, such as coordinate measuring machine (CMM) inspection, to measure the machined parts and decide conformance or non-conformance to specifications [4]. CMMs



Moschos Papananias moschos.papananias@brunel.ac.uk

Department of Mechanical and Aerospace Engineering, Brunel University London, Kingston Lane, Uxbridge, Middlesex UB8 3PH, UK

are one of the most important dimensional metrology equipment for manufacturing quality control due to their accuracy and flexibility in measuring complex parts with a wide range of part and feature characteristics using different sensor technologies [5]. However, they are often a bottleneck to production, particularly conventional CMMs that require stable temperature-controlled conditions to perform consistently [6]. With advances in sensing and computing technologies, the manufacturing industry is entering a new era, known as Industry 4.0, which is characterized by emerging technologies, such as cyber-physical systems (CPSs), the internet of things (IoT), artificial intelligence (AI), and cloud computing [7]. Real-time process and product quality monitoring using data-driven modelling techniques constitutes a key part of the concept of Industry 4.0 to minimize non-valueadding processes, production bottlenecks, re-work, scrap, and cost [8]. Such methods typically rely on digital signal processing and statistical machine learning modelling for fault detection and diagnosis [9]. To achieve this, various sensing techniques have been applied over the years in the area of machining process monitoring [10]. Nevertheless, the overwhelming majority of machining process monitoring methods, particularly for product health prediction, relies on high-cost and intrusive instrumentation, such as dynamometers, which prevents industrial deployment. Therefore, considerable effort has been devoted to developing more practical and flexible monitoring methods for machining processes, suitable for a range of applications with different machining process setups and machine tool access limitations [11].

In terms of monitoring system objectives, many research efforts have been directed towards the application of machine learning modelling algorithms to predicting tool wear [12, 13], chatter [14, 15], and surface roughness [16, 17]. By contrast, much less attention has been paid to map machining process features to dimensional metrology characteristics [18]. This paper presents a multi-sensor machining process monitoring method for product health prediction based on probabilistic machine learning using Gaussian process regression (GPR). Unlike previous approaches, however, the present works rely on a non-intrusive and low-cost instrumentation and data acquisition (DAQ) solution that is flexible in configuration and can be extended with plugand-play simplicity with further measurement modules for different applications with mixed sensor types and sampling rates. The proposed method is tested on a milling case study where it is required to estimate the machined part quality for a specific dimensional quality characteristic (diameter deviation) with acoustic emission (AE) and vibrations sensors installed in the work holding. The novelty of the paper lies in the sensing and DAQ setup for dimensional product health monitoring in milling operations and a Bayesian statistical inference methodology for improving posterior product health parameter estimates using new metrological information from on-machine comparator measurement (OMCM). Bayesian methods allow the information gained in one experiment to be taken into account completely in the analysis of another related experiment.

In summary, the main contributions of the paper include the following:

- The development of an intelligent, probabilistic product health monitoring method based on GPR for machining processes using non-intrusive instrumentation.
- The use of the machine tool as a comparative coordinate measuring system (CMS) is proven to be effective in improving product health metric deviation estimates from probabilistic machine learning via Bayesian inference unlike absolute/traditional on-machine measurements (OMMs).
- Posterior distributions are obtained as a precisionweighted average of the prior and likelihood obtained by probabilistic machine learning and OMCM, respectively.

The remainder of the article is organized as follows: Sect. 2 presents related work on machining process monitoring for a range of scopes. Sections 3 and 4 provide the necessary background on Bayesian inference methodology and GPR. Section 5 presents the experimental work. Section 6 discusses the modelling results obtained by the proposed Bayesian product health monitoring method. Section 7 draws conclusions and provides suggestions for future work.

2 Literature review

In traditional manufacturing, the geometric information of the required workpiece features is typically evaluated using post-process inspection approaches, such as CMM inspection. CMMs are flexible and accurate measuring instruments, and they can deliver improved process productivity and reduced scrap. However, CMM inspection often acts as a bottleneck in the manufacturing process and as an endof-line process does not intrinsically add any value to the manufactured parts, while increasing production time and cost [18]. Computer numerically controlled (CNC) machine tools can also be used as CMSs by exchanging the cutting tool for a machine tool probe. On-machine probing (OMP) is a major in-process inspection approach that can be used to reduce variation sources inherent to machining, such as effects of tool wear on the workpiece and temperature variation, enabling in-process feedback, and provide confidence in the stability of the machining process. The main disadvantage however is that the inspection of machined parts using OMP is sensitive only to errors that are not common to both the machining process and the inspection process as



the same machine is used for both processes. Hence, with OMP, errors, such as machine tool geometry errors, thermal distortions, and errors in thermal corrections applied to the machine tool, cannot be detected [5, 19].

In the high-value manufacturing (HVM) sector, increasingly manufacturers are investing in digital technologies emerging from Industry 4.0 to increase efficiency and productivity in order to stay competitive. A major goal of Industry 4.0 is to reduce redundant processing by developing intelligent process monitoring and control systems with dynamic learning features. Indeed, the research area of manufacturing informatics for autonomous process fault and defect detection embedded within the production cycle is currently developing at an unprecedented rate. Manufacturing informatics is largely aimed at developing new methods that provide effective feedback to the production loop and enhance manufacturing intelligence and autonomy using emerging technologies, such as AI, big data, and dynamic data-driven algorithms. Therefore, real-time process and product health monitoring and control systems for machining operations are crucial in developing processes that yield more precise parts more rapidly with lower manufacturing costs. However, this is highly challenging owing to the complexity of machining processes and the high volumes of data which are being generated by different measurement equipment and processes.

Over the years, several methods have been proposed to monitor machining processes using a range of sensors, such as current/power, dynamometers, accelerometers, AE, and microphones, for a range of monitoring scopes [20]. In this context, Marinescu and Axinte [21] demonstrated the effectiveness of AE signals in monitoring process malfunctions, such as tool defects and workpiece surface anomalies, in milling operations. Wang et al. [22] used a low-cost smart cutting tool to measure cutting forces during machining and adapt the feed rate. Bernini et al. [23] presented a robust unsupervised strategy for milling tool wear monitoring under variable process parameters and lubrication conditions using cutting force signals. McLeay et al. [24] developed and validated an unsupervised machine learning method to observe changing machining process conditions over time in order to detect faulty process conditions, such as worn tools and changes to depth of cut, using non-intrusive sensing. Moore et al. [25] used two tri-axial accelerometers, mounted on the spindle column and bed of the machine tool, respectively, and a power transducer, to assess the machine tool and process condition by applying various machine learning techniques. Plaza et al. [26] examined different signal feature extraction methods to optimize surface finish monitoring using a tri-axial accelerometer mounted on the tip of the tool holder behind the insert. Kovac et al. [27] applied fuzzy logic and regression analysis for modelling surface roughness in dry face milling operations using cutting parameters

and tool wear. Huang [28] proposed a neural-fuzzy inference system for surface roughness prediction in end milling operations using process parameters and cutting force signals. Vasconcelos et al. [29] demonstrated the importance of training machine learning models with both controllable factors and noise variables, such as tool wear, by applying various learning algorithms, including support vector machines, decision trees, and random forest, for surface roughness prediction in milling operations. Decision trees are interpretable machine learning models, but they are prone to overfitting. A solution for nonlinear interpretable input-output mappings has been reported in [30] for areal surface metrology informatics using fuzzy-based machine learning modelling with a ridge penalty term to avoid overfitting of the training model. Furthermore, deep learning algorithms have been applied with great success to machining monitoring tasks [31–34]. Deep learning is a type of machine learning that can achieve state-of-the-art accuracy and flexibility, assuming that large amounts of labelled data and significant computing power are provided. Most deep learning methods are based on artificial neural network (ANN) architectures and stochastic gradient descent optimization [35]. Carbone et al. [36] presented a deep learning approach for machined surface classification tasks using a limited training dataset of optimal and undesired cutting conditions. Wu et al. [37] presented a physics-informed deep learning method for modelling surface roughness in milling operations using cutting force data, machining parameters, tool type, and workpiece properties.

In the context of nonlinear nonparametric solutions, GPR models have been used in several manufacturing applications, such as milling [38], turning [13], multistage manufacturing [39], robotic machining [40], additive manufacturing [41], and semiconductor manufacturing [42], due to their modelling flexibility and inherent capability to provide predictions with estimates of uncertainty. Gaussian processes (GPs) require a suitable covariance kernel function parametrized by a set of hyperparameters to estimate posterior distributions over the function of interest from the training samples [43, 44]. The hyperparameters can be estimated from the data, or they can be fixed. Kong et al. [13] applied GPR for tool wear prediction in turning using cutting force signals and machining parameters. Lu et al. employed GPR for surface roughness prediction in milling using cutting parameters. Song et al. [45] developed a multi-kernel GP autoregressive regression model based on a two-step feature-integration approach to predict both surface roughness and tool wear in milling using cutting force and vibration signals. Qiang et al. [46] applied GPR for tool wear prediction in milling using the net cutting power consumption. Zhao et al. [47] used multi-output GPs and spherical mapping to model 3D surfaces and monitor the geometrical deviations of surfaces. Although GPR models can handle covariates of arbitrary dimension, an important step to consider when

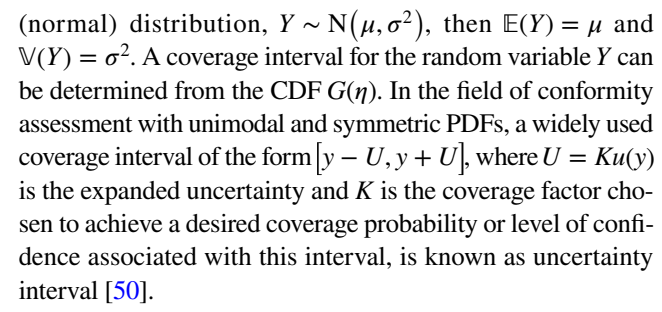


building a model is selecting the covariates that are related to the response variable because this can reduce the complexity of the model and improve its generalization performance. A common method for variable selection in GPR with certain covariance functions is the automatic relevance determination (ARD), but penalized techniques are more flexible and efficient [44].

To summarize, accurately predicting the dimensional end product quality during manufacturing has substantial benefits in terms of productivity, quality, and cost. However, most of the published work focused on the prediction of tool condition/wear and surface metrology parameters, such as surface roughness, using intrusive measurement equipment, and only a few studies have previously applied non-intrusive sensing for machining process monitoring. With the growing demands of developing practical machining process monitoring systems, this paper presents a non-intrusive monitoring method for machining processes using GPR for dimensional end product quality estimation with uncertainty information and a Bayesian statistical inference methodology for providing improved product health parameter estimates given new information from OMCM. Previous studies [39, 48] focused on combining new metrological information from OMP with posterior predictive distributions from probabilistic machine learning have not considered the intrusive nature of sensing used and the influence of systematic effects associated with OMP.

3 Bayesian inference in dimensional metrology

Let Y be a measurand (e.g. diameter) regarded as a continuous random variable with probability density function (PDF) $g(\eta)$, where $\eta \in \mathbb{R}$ is a possible value of Y, $g(\eta) \ge 0 \ \forall \ \eta$ and $\int_{\eta \in \mathbb{R}} g(\eta) d\eta = 1.$ The cumulative distribution function (CDF) of Y, $G(\eta) = P(Y \le \eta)$, gives the probability that the random variable Y is no greater than η , with $G(-\infty) = 0$ and $G(\infty) = 1$, and it can be expressed in terms of the PDF as $G(\eta) = \int_{-\infty}^{\eta} g(t)dt$, $\forall \eta$, where t denotes the variable of integration. If $g(\eta) = dG(\eta)/d\eta$ is the PDF of Y, then the probability of η lying in an interval $[\eta_a, \eta_b]$, with $\eta_a < \eta_b$, is $P(\eta_a \le Y \le \eta_b) = \int_{\eta_b}^{\eta_b} g(\eta) d\eta = G(\eta_b) - G(\eta_a)$. Two important summary statistics of probability distributions are the mean or expectation, which is a measure of location of Y, and the standard deviation (positive square root of the variance), which is a measure of dispersion and referred to as the standard uncertainty u(y) associated with the expectation or an estimate y of Y in the guide to the expression of uncertainty in measurement (GUM) [49]. The expectation of Y with PDF $g(\eta)$ is defined as $\mathbb{E}(Y) = y = \int \eta g(\eta) d\eta$ and the variance as $\mathbb{V}(Y) = \sigma^2 = \int (\eta - y)^2 g(\eta) d\eta$. Note that if Y has a Gaussian



In Bayesian statistical inference, the parameters to be estimated are treated as random variables rather than fixed constants as in frequentist statistical inference. In a Bayesian formulation, knowledge about the measurand Y before a measurement experiment is encoded in a prior PDF $p(\eta|I)$, where I denotes the prior information. Once a measurement experiment has yielded a particular realization η_e , Bayes' theorem can be applied to obtain the posterior distribution of Y:

$$p(\eta|\eta_{e},I) = \frac{p(\eta,\eta_{e}|I)}{p(\eta_{e}|I)} = Cp(\eta|I)p(\eta_{e}|\eta,I), \tag{1}$$

where $p(\eta_e|\eta,I)$ is the likelihood function considered as a function of an assumed value η since a realization η_e exists and $C^{-1} = p(\eta_e|I) = \int p(\eta|I)p(\eta_e|\eta,I)d\eta$ such that $\int p(\eta|\eta_e,I)d\eta = C \int p(\eta|I)p(\eta_e|\eta,I)d\eta = 1$. Hence, Bayes' theorem may be expressed in the form:

$$p(\eta|\eta_e, I) \propto p(\eta|I)p(\eta_e|\eta, I),$$
 (2)

which omits the constant of proportionality, and essentially states that the posterior PDF is proportional to the prior PDF times the likelihood function [51]. The form of likelihood function, $p(\eta_e|\eta, I)$, typically depends on knowledge of the measurement process. Bayes' theorem allows us to combine information from different sources into the posterior PDF, $p(\eta|\eta_e, I)$, which represents all the information about the unknown characteristic parameters taking into account the measurement data and the prior information. In conformity assessment, summary information about the posterior PDF is usually required, particularly the mean and standard deviation of the posterior. Informative prior distributions are used to express the available prior knowledge. If prior knowledge is not available, then a so-called noninformative prior distribution is used. If the prior distribution is normal and the likelihood function can be approximated by a normal distribution, then the posterior is also a normal distribution. Let $\eta_e \sim N(\eta, \sigma_e^2)$ with σ_e^2 known. If $\eta \sim N(\mu_0, \sigma_0^2)$ is the prior distribution for η , then the posterior of η is a normal density with mean η_1 and variance σ_1^2 :

$$\eta_1 = \frac{\mu_0 \sigma_0^{-2} + \eta_e \sigma_e^{-2}}{\sigma_0^{-2} + \sigma_e^{-2}}, \sigma_1^2 = \left(\sigma_0^{-2} + \sigma_e^{-2}\right)^{-1}.$$
 (3)



4 Gaussian process regression

GPs are a flexible class of non-parametric kernel-based probabilistic machine learning models that have been applied extensively to regression problems [43]. Consider a training dataset $D = \{(\mathbf{x}_i, h_i) | i = 1, ..., m\}$, drawn from

$$h_i = f(\mathbf{x}_i) + \epsilon_i, \tag{4}$$

where $\mathbf{x}_i \in \mathbb{R}^n$ is a vector of predictors, f is an unknown function, $h_i \in \mathbb{R}$ is a scalar response (target), and ϵ_i is a Gaussian measurement noise with zero mean and variance σ_ϵ^2 , $\epsilon_i \sim \mathrm{N}(0,\sigma_\epsilon^2)$. GP modelling is a Bayesian non-parametric approach that defines a GP, parametrized in terms of a mean function, $\psi(\mathbf{x}) = \mathbb{E}(f(\mathbf{x}))$, and a covariance function (kernel), $k(\mathbf{x}, \mathbf{x}') = \mathrm{cov}(f(\mathbf{x}), f(\mathbf{x}'))$, as a prior distribution for $f(\mathbf{x})$:

$$f(\mathbf{x}) \sim \mathcal{GP}(\psi(\mathbf{x}), k(\mathbf{x}, \mathbf{x}')).$$
 (5)

It is common to assume that the prior mean function is zero if there is no prior information about the mean function of the GP. The covariance function, $k(\mathbf{x}, \mathbf{x}')$, depends on the inputs \mathbf{x} and \mathbf{x}' and the choice of the kernel function with hyperparameters θ , which can be estimated from the data, $D = \{X, h\}$, where $\mathbf{X} = (\mathbf{x}_1, \dots, \mathbf{x}_m)^{\mathrm{T}} \in \mathbb{R}^{m \times n}$ denotes the matrix of predictors and $\mathbf{h} = (h_1, \dots, h_m)^{\mathrm{T}} \in \mathbb{R}^{m \times 1}$ the corresponding response vector. The conditional distribution of h given f and σ_{ϵ}^2 is multivariate Gaussian, $h|f, \sigma_{\epsilon}^2 \sim N_m(h|f, \sigma_{\epsilon}^2 \mathbf{I})$, where \mathbf{I} is the $m \times m$ identity matrix and $f = (f(\mathbf{x}_1), \dots, f(\mathbf{x}_m))^{\mathrm{T}} \in \mathbb{R}^{m \times 1}$, is the vector of latent variables with $f_i = f(\mathbf{x}_i)$. The vector of latent function values fhas a multivariate Gaussian distribution, $f|\mathbf{X}, \theta \sim N_m(f|\mathbf{0}, \mathbf{K})$, where $\mathbf{0}$ is the m-dimensional mean vector of all zeros and $\mathbf{K} = \left[k(\mathbf{x}_i, \mathbf{x}_j) \right]_{\forall i,j}$ is the $m \times m$ covariance matrix evaluated at all pairs of the *m* training points, $\{k(\mathbf{x}_i, \mathbf{x}_i) | i, j = 1, ..., m\}$, using a particular form of covariance function with hyperparameters θ . The most widely used covariance function is the squared exponential (SE):

$$k_{SE}(\mathbf{x}_i, \mathbf{x}_j | \boldsymbol{\theta}) = \sigma_f^2 \exp \left[-\frac{\left| \mathbf{x}_i - \mathbf{x}_j \right|^2}{2l^2} \right], \tag{6}$$

where σ_f (scaling parameter) and l (characteristic length-scale) are hyperparameters, which control the magnitude and the smoothness of the function, respectively, and $\left|\mathbf{x}_i - \mathbf{x}_j\right|^2$ is the squared Euclidean distance between the predictor variables \mathbf{x}_i and \mathbf{x}_j . Since the likelihood, $p(\mathbf{h}|\mathbf{f}, \sigma_\epsilon^2)$, and the prior, $p(\mathbf{f}|\mathbf{X}, \boldsymbol{\theta})$, are both multivariate Gaussian, the posterior distribution of the vector of latent function values \mathbf{f} is also multivariate Gaussian:

$$f|\mathbf{X}, \boldsymbol{h}, \boldsymbol{\theta}, \sigma_{\epsilon}^{2} \sim N_{m} \Big(\mathbf{K} \Big(\mathbf{K} + \sigma_{\epsilon}^{2} \mathbf{I} \Big)^{-1} \boldsymbol{h}, \sigma_{\epsilon}^{2} \mathbf{K} \Big(\mathbf{K} + \sigma_{\epsilon}^{2} \mathbf{I} \Big)^{-1} \Big).$$
(7)

Thus, the GP posterior at a test input \mathbf{x}_* is Gaussian, $f_*|\mathbf{X}, \boldsymbol{h}, \boldsymbol{\theta}, \sigma_e^2, \mathbf{x}_* \sim N(\overline{f}_*, \sigma_*^2)$ with posterior predictive mean and variance:

$$\bar{f}_* = \mathbb{E}(f_*) = \mathbf{k}_*^{\mathrm{T}} (\mathbf{K} + \sigma_c^2 \mathbf{I})^{-1} \boldsymbol{h}, \tag{8}$$

and

$$\sigma_*^2 = \mathbb{V}(f_*) = k(\mathbf{x}_*, \mathbf{x}_*) - \mathbf{k}_*^{\mathrm{T}} (\mathbf{K} + \sigma_e^2 \mathbf{I})^{-1} \mathbf{k}_*$$
 (9)

respectively, where $\mathbf{k}_* = \begin{bmatrix} k(\mathbf{x}_*, \mathbf{x}_i) \end{bmatrix}_{\forall i}^{\mathsf{T}}$ is the $m \times 1$ vector of covariances between the test point \mathbf{x}_* and the m training points, $\left\{ k(\mathbf{x}_*, \mathbf{x}_i) | i = 1, \ldots, m \right\}$. Hence, the predictive distribution of h_* is Gaussian with mean $\mathbb{E} \left(f_* \right) = \mathbb{E} \left(h_* \right)$ and variance $\widehat{\sigma}_*^2 = \mathbb{V} \left(h_* \right) = \mathbb{V} \left(f_* \right) + \sigma_\epsilon^2$. Given that $h \sim \mathrm{N}_m \left(\mathbf{0}, \mathbf{K} + \sigma_\epsilon^2 \mathbf{I} \right)$, the hyperparameters θ and noise variance σ_ϵ^2 of the GP model can be estimated by maximizing the marginal likelihood $p(h|\mathbf{X})$ as a function of θ and σ_ϵ^2 , i.e., $\widehat{\theta}, \widehat{\sigma}_\epsilon^2 = \underset{\theta, \sigma_\epsilon^2}{\operatorname{argmax}} \log p\left(h|\mathbf{X}, \theta, \sigma_\epsilon^2 \right)$. The log marginal likelihood is given by

$$\log p(\boldsymbol{h}|\mathbf{X}, \boldsymbol{\theta}, \sigma_{\epsilon}^{2}) = -\frac{1}{2}\boldsymbol{h}^{\mathrm{T}} (\mathbf{K} + \sigma_{\epsilon}^{2}\mathbf{I})^{-1}\boldsymbol{h} - \frac{1}{2}\log \left|\mathbf{K} + \sigma_{\epsilon}^{2}\mathbf{I}\right| - \frac{m}{2}\log(2\pi).$$
(10)

5 Experimental approach and setup

A major obstacle in product quality monitoring research for machining processes is the lack of a non-intrusive and lowcost multi-sensor system that is straightforward to install, configure, and extend with further measurement modules for different industrial manufacturing applications. An EMCO MAXXMILL 350 vertical milling centre was used in the experimental trials for machining holes under dry conditions with process variability added through different feed rates and spindle speeds. In particular, a full factorial design was performed with two factors (feed rate and spindle speed) at three levels each (400, 420, and 440 mm/min, and 1592, 1672, and 1752 rev/min, respectively). The workpiece material used throughout the tests was EN3B engineering steel due to its low cost and use in a variety of applications, such as machinery parts. An indexable milling cutter with three interchangeable inserts having two helical cutting edges (APKT 1003PDTR-76 IC328) suitable for many applications on steel and stainless steel and interrupted cuts and milling under unstable conditions was employed for the experiment. The inserts were replaced (or rotated to another cutting edge) at irregular intervals to add further variability in the data and represent industrial cutting conditions. In total, 486 holes



were milled using three replicates of the experimental design (27 parts with 18 holes each from both sides of the workpiece). The study in this paper utilized 22 parts (396 holes) from this experimental design.

The monitoring system for product health prediction included a number of different sensors: a passive piezoelectric AE sensor (Vallen Systeme VS150-K3) with a frequency range (Fpeak) of 100-450 kHz (150 kHz), a triaxial accelerometer (PCB 604B31) with a frequency range (\pm 3 dB) of 0.5-5000 Hz, a uniaxial accelerometer (PCB 352A60) with a frequency range (±3 dB) of 5-60,000 Hz, and a microphone system (PCB 378C01), which was excluded for this study. The experimental data were obtained using a National Instruments USB Compact DAQ Chassis (NI cDAQ-9174) with different voltage input modules, including the NI-9223 and the NI-9775. Regarding the sensor signal conditioners, a PCB 482C05 4-channel signal conditioner was employed for both accelerometers and an AEP5 pre-amplifier with a DCPL2 decoupling box for the AE sensor. In this study, all sensor signals were measured simultaneously at 500 kHz during milling, allowing frequency content up to 250 kHz to be observed. The NI LabVIEW SignalExpress software was used for acquiring the AE and vibration signals, which provides both the original signals and the corresponding decimated data at different levels though M-fold decimation preceded with lowpass finite impulse response (FIR) filtering to prevent aliasing from occurring due to the lower sampling frequencies. All the sensors were installed in the machine vise using magnetic holders.

After machining, OMP was performed using the Renishaw OMP 40-2 optical inspection probe system whose measurement repeatability is 1 μ m 2 σ . The measuring cycles were produced using the Renishaw Inspection Plus software for machining centres for Siemens Controllers. The measurand of interest in this study is the diameter of the machined holes. Four contact points were selected to be taken for each milled hole. For post-process inspection, a Mitutoyo CMM, equipped with MCOSMOS software, was used in laboratory

conditions to measure the milled holes. The probe system used was the Renishaw SP25M, which can function either as a scanning probe or as a touch-trigger probe. In this study, the probe was used in touch-trigger probing mode where four discrete points were taken for each milled hole measured as such a sample size of probing points is sufficient for this geometric feature and it is practical for a production setting. In total, 396 diameter measurements were determined from each inspection approach, but both approaches were also repeated under different conditions on a set of test parts for the experimental assessment of uncertainty. In addition, an additional part to be used as a master part for comparator measurements was produced and measured by both inspection approaches. The whole experiment was carried out at the University of Portsmouth. The experimental setup can be seen in Fig. 1.

6 Probabilistic product health monitoring using non-intrusive sensing and OMCM

The datasets utilized in this study include the first level of decimated machining process monitoring data, the in-process inspection data, and the post-process inspection data. MATLAB was used for all computations, including signal segmentation, feature generation, machine learning, and Bayesian inference. Segmentation was applied to the decimated signals in order to remove the non-cutting condition data. After signal segmentation, the following time-domain features were computed: the mean, standard deviation, root mean square (RMS), kurtosis, skewness, shape factor, peak value, clearance factor, crest factor, impulse factor, signalto-noise ratio (SNR), and signal-to-noise-and-distortion ratio (SINAD). The extracted process features were used as inputs to the GPR model, along with the corresponding cutting parameters. The predictors were standardized using their corresponding means and standard deviations. Figure 2 shows an example of AE data for selected pairs

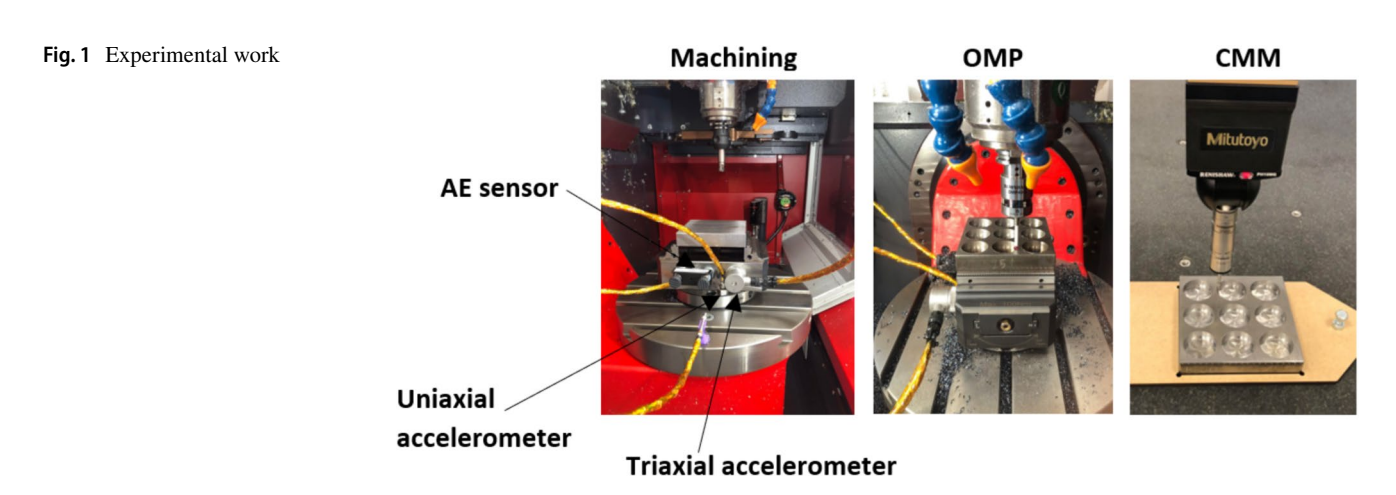




Fig. 2 Bivariate histogram plots of selected time-domain AE features

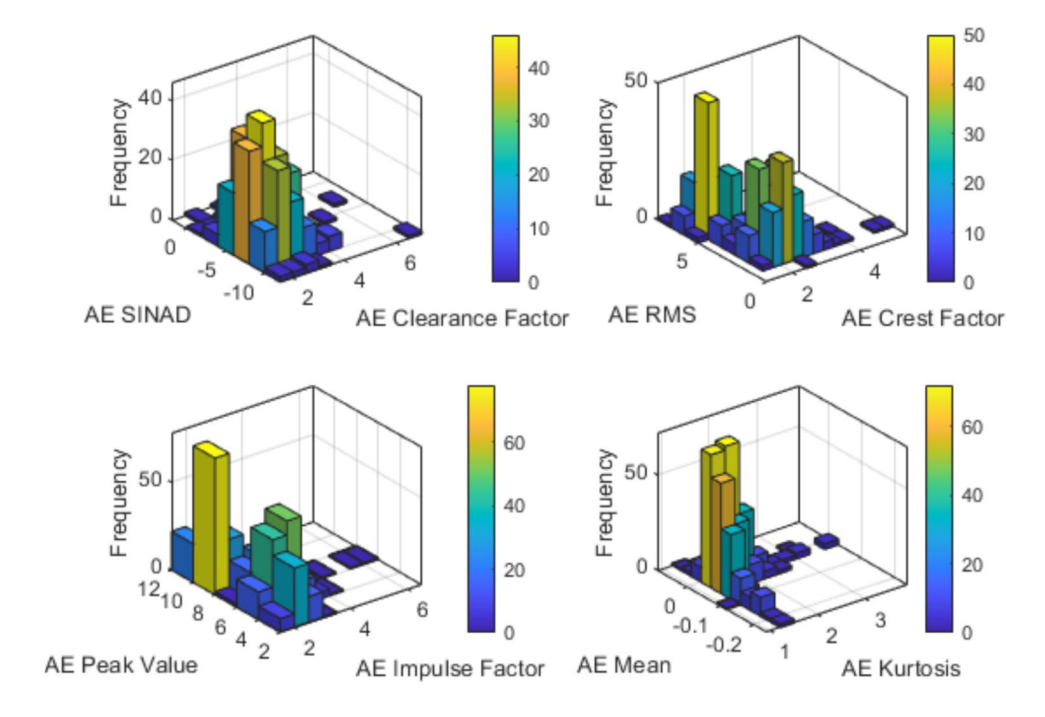
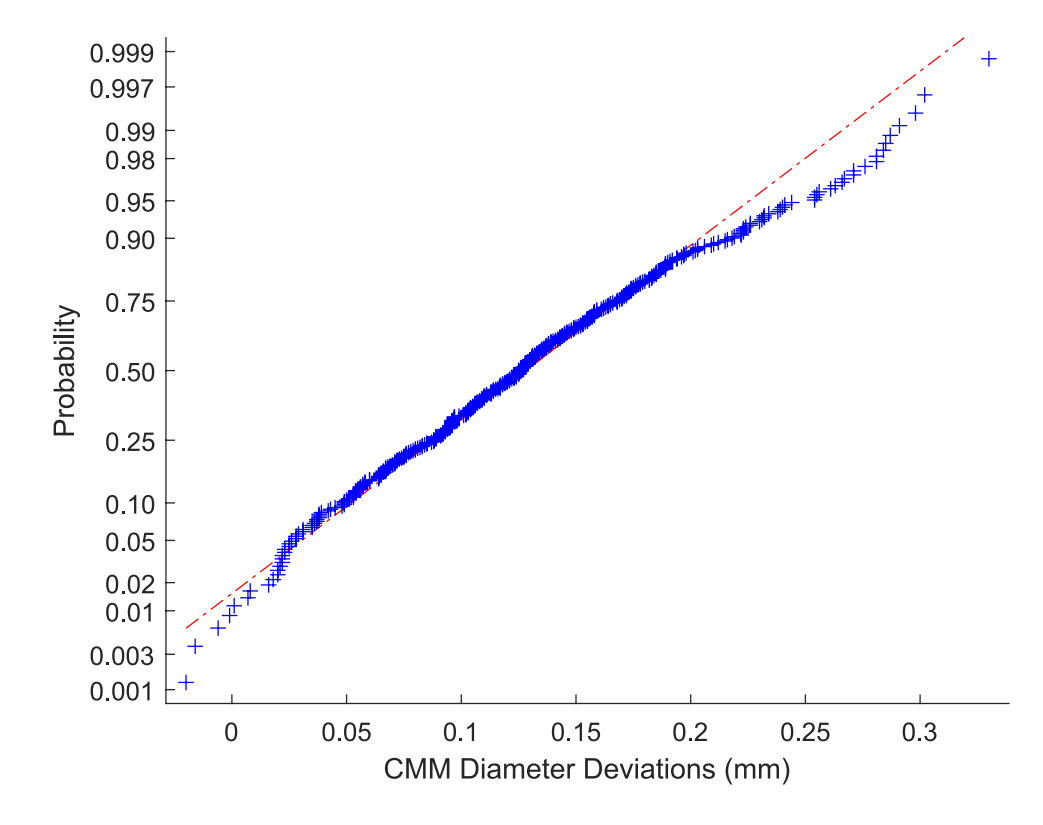


Fig. 3 Normal probability plot of the CMM measured deviations



of features using bivariate histograms. The CMM product health metric deviations, $h_{\rm e}=h_{\rm m}-\widetilde{y}$, were used as output data, where $h_{\rm m}$ is the CMM measured value and $\widetilde{y}=35{\rm mm}$ is the nominal diameter value. Figure 3 shows the normal probability plot of the output data, indicating that the data are normally distributed with non-substantive deviation from normality given the high variability of the data in this

study. CMM inspection experiments were carried out under repeatability and reproducibility conditions to evaluate the uncertainty associated with CMM measurement.

The dataset was randomly split into a training set, containing 90% of the dataset, and a reserved test set containing the remaining 10%. Automatic relevance determination (ARD) was used to select an optimal subset of covariates



from the model. This typically improves the model's performance and reduces its complexity. The ARD-SE kernel is defined by

$$k_{ARD-SE}(\mathbf{x}_i, \mathbf{x}_j | \boldsymbol{\theta}) = \sigma_f^2 \exp \left[-\frac{1}{2} \sum_{d=1}^n \frac{\left(\mathbf{x}_{id} - \mathbf{x}_{jd} \right)^2}{l_d^2} \right], \quad (11)$$

where $\theta = (\sigma_f, l_1, \dots, l_n)^{\mathrm{T}}$. The hyperparameter l_d is a characteristic length-scale, which controls the smoothness of the function in the direction of the d-th predictor variable. Therefore, the hyperparameters l_1, \dots, l_n can determine the relevance of the corresponding input variables to the output variable. A major limitation of using GPs for large datasets is that the computational complexity grows at rate $\mathcal{O}(m^3)$ due to the inversion of the $m \times m$ covariance matrix. Several approaches, such as sparse approximations [52–54] and local-expert models [55–57], have been proposed to alleviate their computational cost. However, in the present case study, the available dataset is small enough for an exact implementation without being computationally expensive.

A GPR model using the ARD-SE kernel, which selects an optimal subset of covariates, $\mathbf{x}_i = \left(x_{i1}, \dots, x_{in}\right)^T$, was used for mapping the process conditions to the CMM product health metric deviations. The performance measure utilized to evaluate the proposed GPR model was the root mean squared error (RMSE) because it is easy to interpret. The performance of the model in predicting the diameter deviations is shown in Figs. 4 and 5 for the training and test sets, respectively. As can be noted from the measured vs predicted plots, the model does not overfit on the training set (Fig. 4) and is able to generalize well to unseen data (Fig. 5). Figures 6 and 7 show the CMM measured diameter deviations, the predicted diameter deviations, and the 95% prediction intervals, where it can be seen

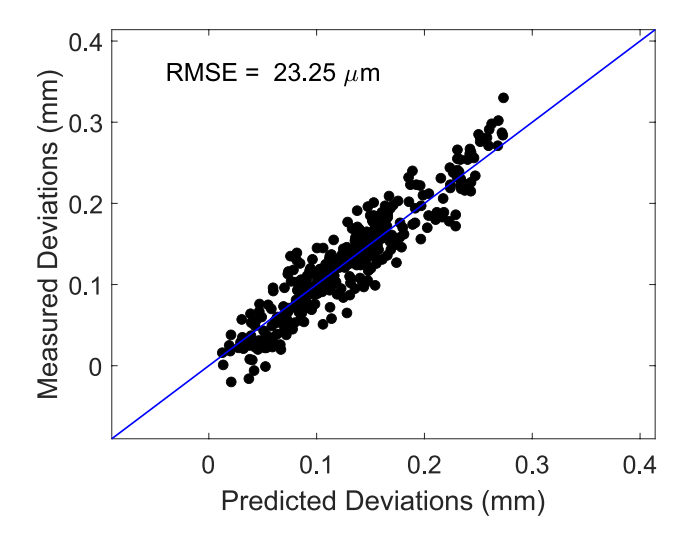


Fig. 4 GPR model performance on the training set



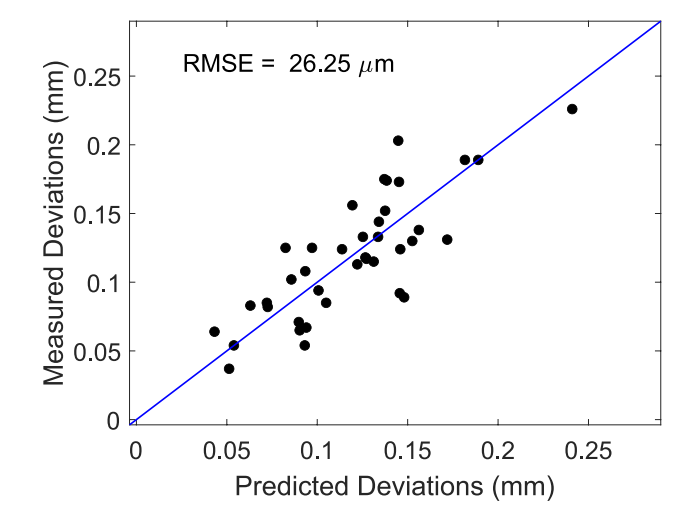


Fig. 5 GPR model performance on the test set

that the developed GPR model yields accurate prediction results with reasonable uncertainty intervals given the large variability of the data. Figure 8 shows the histogram of residuals from both training and testing. In addition, the generalization performance of the GPR model was evaluated using k-fold cross-validation. In particular, a fivefold cross-validation approach was employed, partitioning the dataset into five randomly chosen subsets (folds) of roughly equal size, to iteratively train and test the GPR model. One fold containing 20% of the dataset was used to test the GPR model trained using the remaining folds containing 80% of the dataset. This process was repeated 5 times so that each fold was used as the test set once. The weighted average RMSEs were 0.023mm and 0.028mm for training and testing, respectively. Figures 9 and 10 show the measured vs predicted plots for the training and test sets, respectively, for a randomly chosen fold. However, the proposed probabilistic product health monitoring method can benefit from subsequent information, such as OMP measurements, particularly for GPR prediction results with large uncertainty intervals. In other words, when the GPR model cannot be confident in its predictions, OMP can be performed to improve the prediction results in terms of accuracy and level of uncertainty via Bayesian statistical inference. In this study, both sources of information can be well represented with normal densities. Thus, the posterior distribution of product health metric deviation estimates given in-process monitoring and in-process inspection data can be represented as a compromise between the predicted response from the GPR model and the observed OMP value or maximum likelihood estimate, which is simply the sample mean, for multiple OMP observations on the same feature of the part. Hence, the resulting posterior for diameter deviation estimates will also be a normal density, with a mean equal to a precision-weighted average of the GPR

Fig. 6 GPR model prediction results on the training set

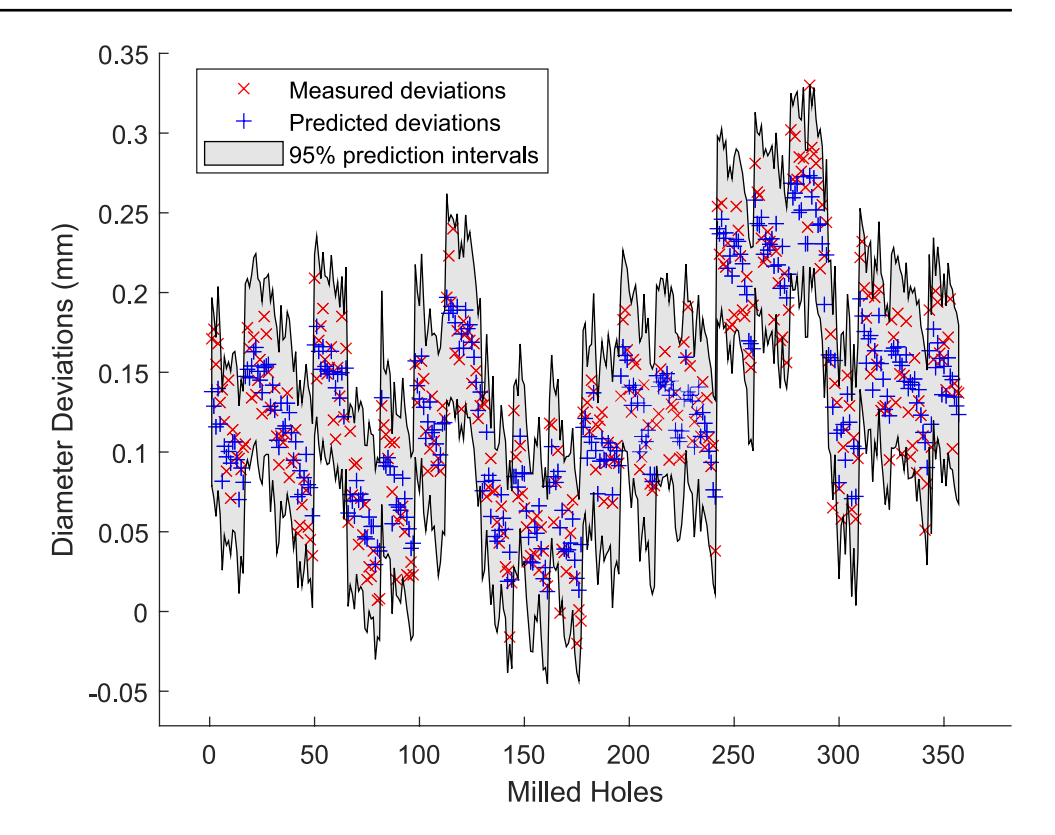
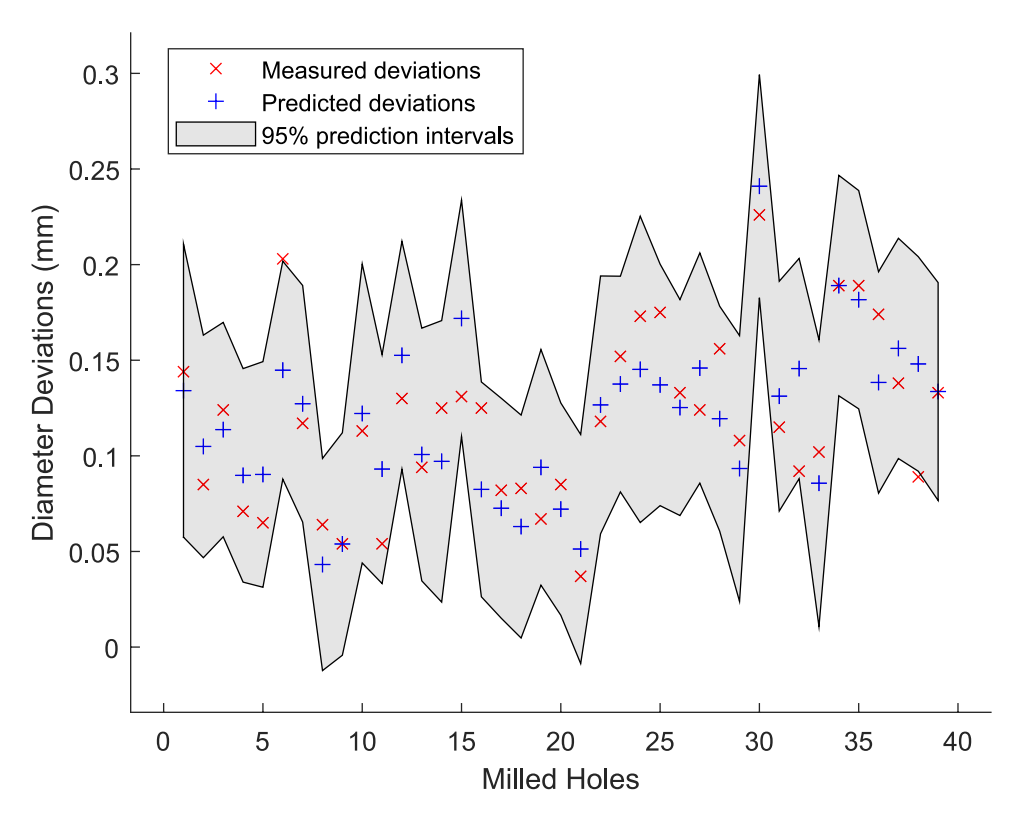


Fig. 7 GPR model prediction results on the test set



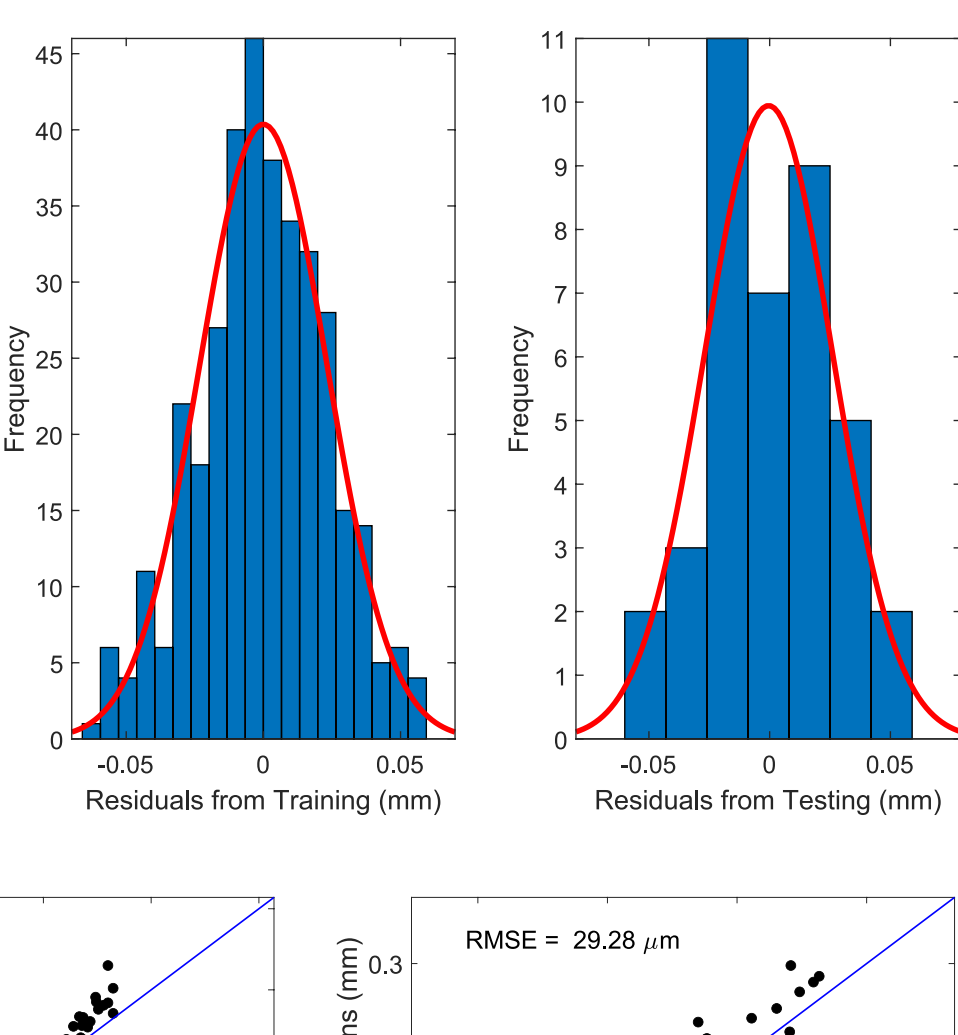
posterior predictive mean and the corresponding observed OMP value or sample mean.

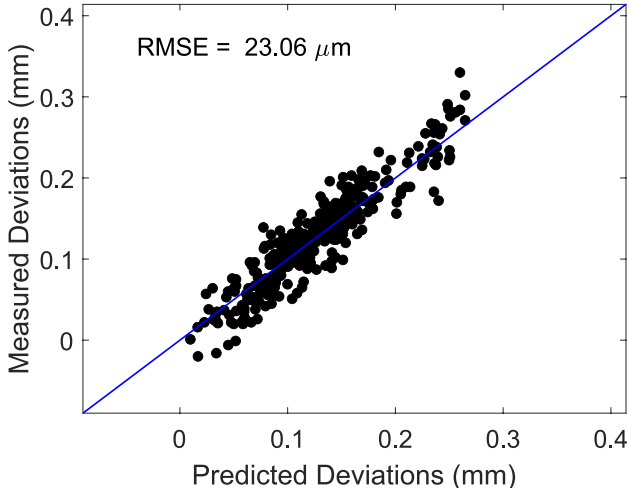
Let $\eta_{\rm e} = \eta_{\rm m} - \widetilde{y}$ be the difference between the OMP measurement, $\eta_{\rm m}$, and the nominal diameter value, \widetilde{y} . Assuming

a normal likelihood for OMP data, $\eta_{\rm e} \sim N(\eta, \sigma_{\rm e}^2)$ with $\sigma_{\rm e}^2$ fixed, a conjugate prior distribution for η is the normal. If $\eta \sim N(\mu_0, \sigma_0^2)$ is the prior distribution for η , where $\mu_0 = \overline{f}_*$



Fig. 8 Histogram of residuals with a normal density fit





0.3 RMSE = 29.28 μm

0 0.1 0.2 0.3 Predicted Deviations (mm)

Fig. 9 GPR model performance on the training set for a randomly chosen fold from fivefold cross-validation

Fig. 10 GPR model performance on the test set for a randomly chosen fold from fivefold cross-validation

and $\sigma_0^2 = \widehat{\sigma}_*^2$, then the posterior for η , $p(\eta|\eta_e,I)$, where I includes the known variance σ_e^2 , is a normal density with mean $\eta_1 = \eta_e + w(\mu_0 - \eta_e), w = \sigma_0^{-2}/(\sigma_0^{-2} + \sigma_e^{-2}) \in (0,1)$, and variance $\sigma_1^2 = (\sigma_0^{-2} + \sigma_e^{-2})^{-1}$. However, notice that the resulting posterior may lead to improved or reduced product health parameter estimates depending on whether OMP provides new accurate information or not. This is illustrated in Fig. 11 where the resulting posterior distribution is shifted away from the

target (CMM) distribution. OMP can be used with a comparator method to correct for the systematic effects associated with OMM, because major sources of error present during machining are also present during automated probing. To achieve this, first, a master part, nominally of the same design, is calibrated with a Mitutoyo CMM in stable temperature-controlled conditions according to the technical requirements of the application. The calibrated master part is then measured on the



Fig. 11 Bayesian inference for end product condition with OMM

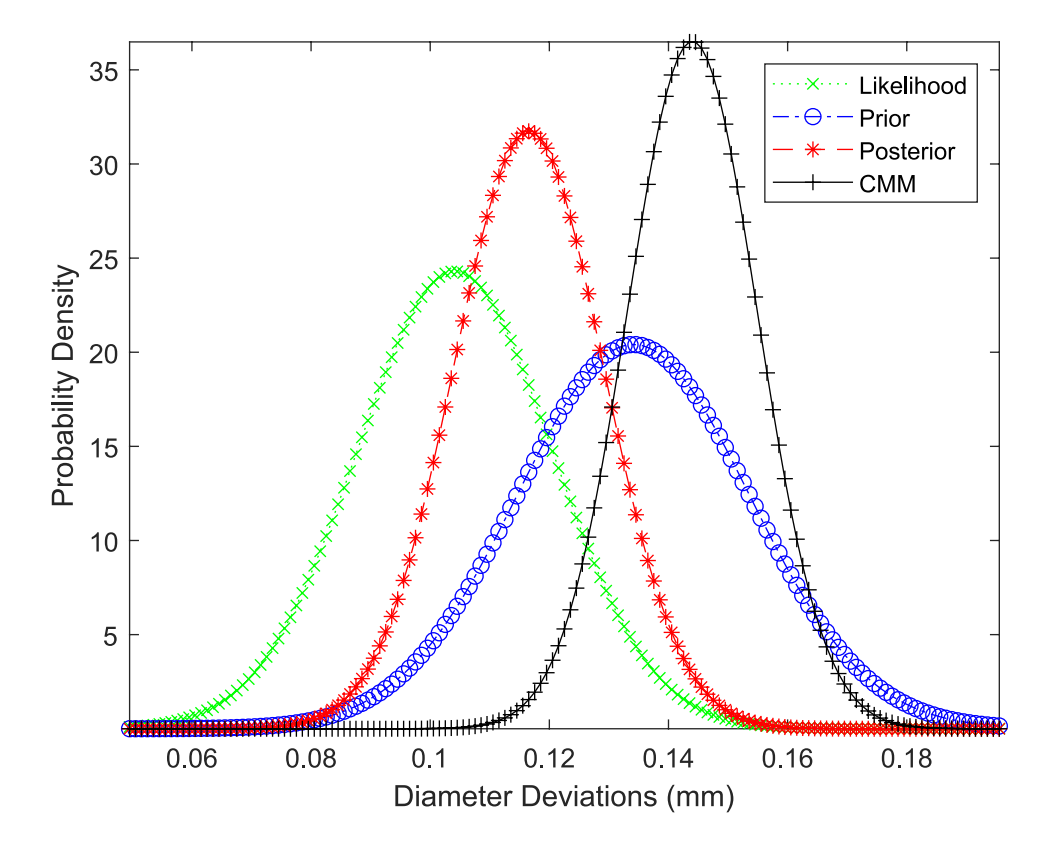


Fig. 12 Bayesian inference for end product condition with OMCM (same part)

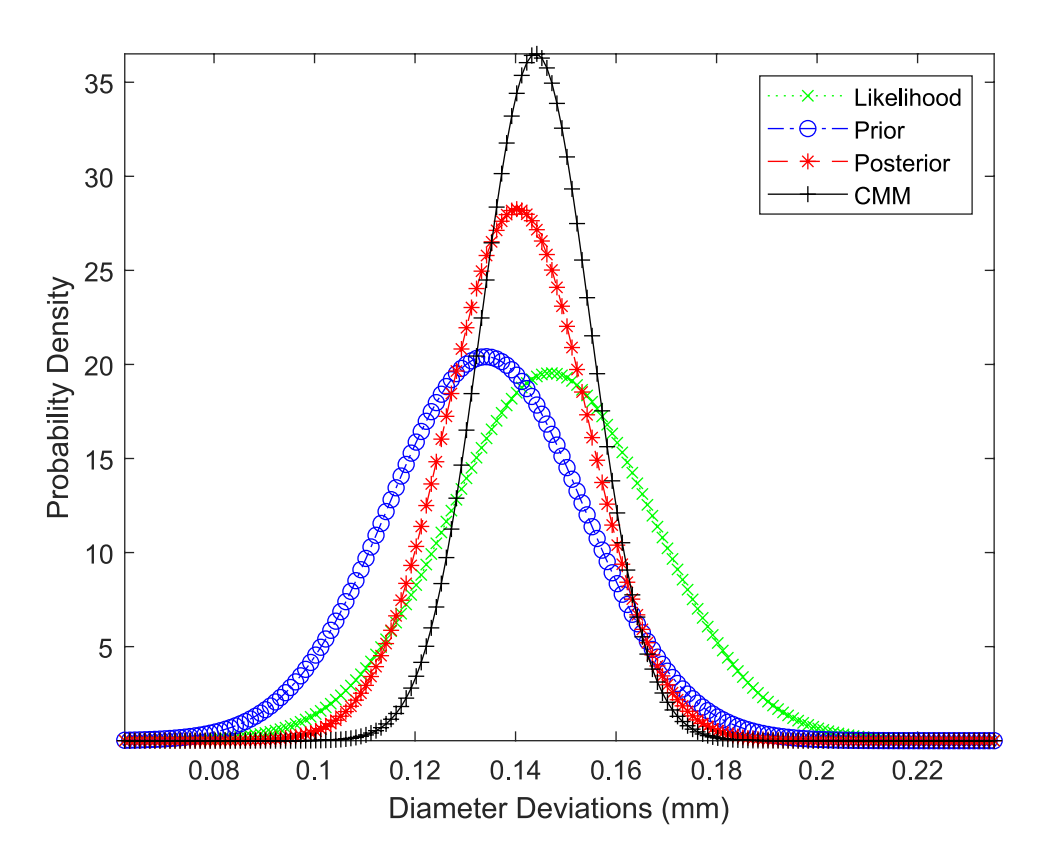
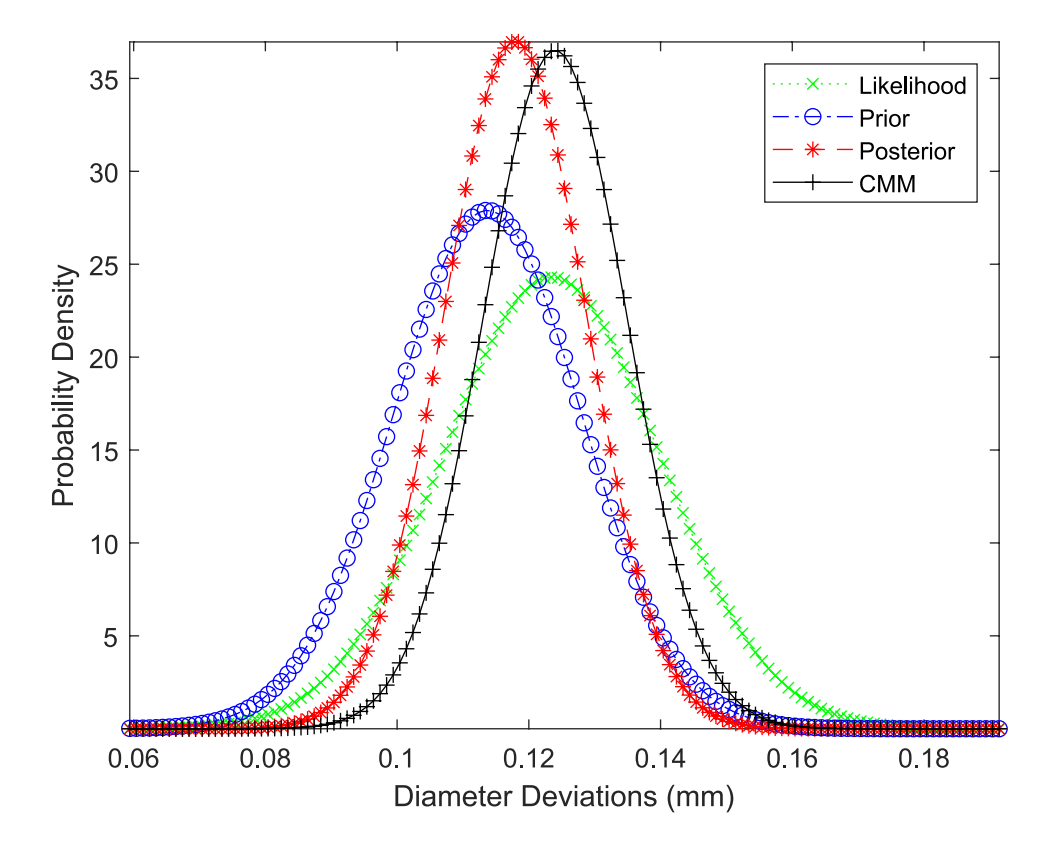




Fig. 13 Bayesian inference for end product condition with OMCM (different part)



machine tool with OMP based on the same measurement strategy, and the uncertainties for both measurement procedures are calculated experimentally. The difference between the measured and calibrated values of the master part, or the difference between the average of the measured values of the master part and the average of the calibrated values of the master part, in the case of repeated measurements, is added as a correction to the OMP observed value of each test part. The systematic error is $c = \eta_{\rm cal} - h_{\rm cal}$, where $\eta_{\rm cal}$ and $h_{\rm cal}$ denote the OMP measured value and the CMM calibrated value of the master part, respectively. When OMP measurement results are corrected by the amount of systematic effects, i.e., $\eta_{\rm m}^* = \eta_{\rm m} - c$, as with CMSs operating in comparator mode, such as automated comparator gauges, the combined uncertainty associated with OMCM should consider the uncertainty parameter obtained by the calibration of the master part, the uncertainty associated with the systematic error evaluated using repeated measurements on the calibrated master part under varying conditions, the uncertainty of the measurement procedure on the test part, and the uncertainty due to material and manufacturing variations [58]. This means that comparator measurement requires subsequent measurements on the calibrated master part at regular time intervals in order to derive an accurate correction value, but a nonlinear probabilistic mapping from in-process inspection conditions to post-process inspection can be found to reduce the volume of additional measurements and receive new calibration information. For modelling purposes, the posterior predictive distribution for a future observation from the model is

treated as the prior, and the new metrological information from OMCM, $\eta_e^* = \eta_m^* - \widetilde{y}$, is treated as the likelihood in the same way as conventional OMP, η_e . As can be seen from the results of Fig. 12 (same part as before) and Fig. 13 (different part), marrying the prior information from the posterior predictive distribution with the new information from OMCM data leads to improved posterior inferences about the end product condition. When the prior information from the posterior predictive distribution for a future observation and the new information from OMCM are in great conflict, then, the target (CMM) and posterior distributions are markedly different from one another, and new calibration information is required to correct for the influence of systematic effects associated with OMP.

7 Conclusions

Despite remarkable research efforts and progress in the development and validation of real-time machining process monitoring systems for various scenarios, their industrial realization is still hampered by several obstacles. A major obstacle to their industrial implementation is the prohibitive cost and intrusive nature of sensors typically used for monitoring machining processes. Although previous studies have presented methods for product quality monitoring, reducing the volume of post-process inspections, the vast majority of applications reported on the use of cutting force, spindle, and tool vibration measurements. Whilst such measurement



signals are particularly useful to infer the process condition and detect non-conforming products, the applicability of this instrumentation in a production scenario is limited. To ensure that the manufacturing industry can adopt a sensorbased monitoring solution for product health prediction, the instrumentation must be non-intrusive to the process.

This paper has presented a new product health monitoring method for machining processes using non-intrusive and low-cost instrumentation and data acquisition (DAO) hardware, which can be extended with different measurement modules. A Gaussian process regression (GPR) model was developed to provide product health metric deviation estimates with uncertainty information using coordinate measuring machine (CMM) and in-process monitoring data, including acoustic emission (AE) and vibration. Also, Bayesian statistical inference was applied to dynamically incorporate new information from on-machine comparator measurement (OMCM) and increase the generalization performance and robustness of the system, providing improved product health parameter estimates during manufacturing. However, the proposed product health monitoring method has also some limitations. Gaussian processes (GPs) have cubic complexity of training, which is prohibitive for large datasets. Thus, one needs approximation schemes to reduce this complexity for modelling problems with large datasets. For variable selection, automatic relevance determination (ARD) was used to remove irrelevant input variables from the model, but penalized regression techniques may be more efficient on variable selection. Therefore, future work will focus on developing a penalized GPR approach for product quality monitoring in machining processes and also look to apply the proposed monitoring method to multi-operation machining processes in the presence of coolant for complex parts with different critical features.

Funding The author gratefully acknowledges the Royal Society for the grant RGS\R2\222098.

Declarations

Competing interests The author declares no competing interests.

Open Access This article is licensed under a Creative Commons Attribution 4.0 International License, which permits use, sharing, adaptation, distribution and reproduction in any medium or format, as long as you give appropriate credit to the original author(s) and the source, provide a link to the Creative Commons licence, and indicate if changes were made. The images or other third party material in this article are included in the article's Creative Commons licence, unless indicated otherwise in a credit line to the material. If material is not included in the article's Creative Commons licence and your intended use is not permitted by statutory regulation or exceeds the permitted use, you will need to obtain permission directly from the copyright holder. To view a copy of this licence, visit http://creativecommons.org/licenses/by/4.0/.

References

- Shi J (2006) Stream of variation modeling and analysis for multistage manufacturing processes. CRC Press, Boca Raton, FL
- Filipovic V, Nedic N, Stojanovic V (2011) Robust identification of pneumatic servo actuators in the real situations. Forsch Ingenieurwes 75:183–196
- Song X et al (2023) Improved dynamic event-triggered security control for T-S fuzzy LPV-PDE systems via pointwise measurements and point control. Int J Fuzzy Syst 25(8):3177–3192
- Forbes AB (2006) Measurement uncertainty and optimized conformance assessment. Measurement 39(9):808–814
- Hocken RJ, Pereira PH (2012) Coordinate measuring machines and systems, 2nd edn. CRC Press, Boca Raton, FL
- Papananias M et al (2017) Uncertainty evaluation associated with versatile automated gauging influenced by process variations through design of experiments approach. Precis Eng 49:440–455
- Lu Y (2017) Industry 4.0: A survey on technologies, applications and open research issues. J Ind Inf Integr 6:1–10
- Papananias M et al (2019) A Bayesian framework to estimate part quality and associated uncertainties in multistage manufacturing. Comput Ind 105:35–47
- Tao H et al (2020) An unsupervised fault diagnosis method for rolling bearing using STFT and generative neural networks. J Frank Inst 357(11):7286–7307
- Teti R et al (2010) Advanced monitoring of machining operations. CIRP Ann 59(2):717–739
- McLeay TE (2016) Unsupervised monitoring of machining processes. Dissertation (PhD Thesis), University of Sheffield
- Karandikar J et al (2015) Tool wear monitoring using naive Bayes classifiers. Int J Adv Manuf Technol 77:1613–1626
- Kong D, Chen Y, Li N (2018) Gaussian process regression for tool wear prediction. Mech Syst Signal Process 104:556–574
- Chen Y et al (2019) Intelligent chatter detection using image features and support vector machine. Int J Adv Manuf Technol 102:1433–1442
- Chen GS, Zheng QZ (2018) Online chatter detection of the end milling based on wavelet packet transform and support vector machine recursive feature elimination. Int J Adv Manuf Technol 95:775–784
- Khorasani A, Yazdi MRS (2017) Development of a dynamic surface roughness monitoring system based on artificial neural networks (ANN) in milling operation. Int J Adv Manuf Technol 93:141–151
- Guo W et al (2021) Prediction of surface roughness based on a hybrid feature selection method and long short-term memory network in grinding. Int J Adv Manuf Technol 112:2853–2871
- Papananias M et al (2020) Inspection by exception: a new machine learning-based approach for multistage manufacturing. Appl Soft Comput 97:106787
- Groover MP (2016) Automation, production systems, and computer-integrated manufacturing, 4th edn. Pearson Higher Education, USA
- Shokrani A et al (2024) Sensors for in-process and on-machine monitoring of machining operations. CIRP J Manuf Sci Technol 51:263–292
- Marinescu I, Axinte DA (2008) A critical analysis of effectiveness of acoustic emission signals to detect tool and workpiece malfunctions in milling operations. Int J Mach Tools Manuf 48(10):1148–1160
- 22. Wang C et al (2013) Adaptive smart machining based on using constant cutting force and a smart cutting tool. Proc Inst Mech Eng Pt B J Eng Manuf 227(2):249–253
- Bernini L, Albertelli P, Monno M (2023) Mill condition monitoring based on instantaneous identification of specific force



- coefficients under variable cutting conditions. Mech Syst Signal Process 185:109820
- McLeay T, Turner MS, Worden K (2021) A novel approach to machining process fault detection using unsupervised learning. Proc Inst Mech Eng Pt B J Eng Manuf 235(10):1533–1542
- Moore J, Stammers J, Dominguez-Caballero J (2021) The application of machine learning to sensor signals for machine tool and process health assessment. Proc Inst Mech Eng Pt B J Eng Manuf 235(10):1543–1557
- Plaza EG, López PN, González EB (2019) Efficiency of vibration signal feature extraction for surface finish monitoring in CNC machining. J Manuf Process 44:145–157
- Kovac P et al (2013) Application of fuzzy logic and regression analysis for modeling surface roughness in face milling. J Intell Manuf 24:755–762
- Huang PB (2016) An intelligent neural-fuzzy model for an inprocess surface roughness monitoring system in end milling operations. J Intell Manuf 27:689–700
- Vasconcelos GAVB et al (2024) Prediction of surface roughness in duplex stainless steel top milling using machine learning techniques. Int J Adv Manuf Technol 133:2031–2048
- Obajemu O et al (2021) An interpretable machine learning based approach for process to areal surface metrology informatics. Surf Topogr Metrol Prop 9(4):044001
- Nasir V, Sassani F (2021) A review on deep learning in machining and tool monitoring: methods, opportunities, and challenges. Int J Adv Manuf Technol 115(9):2683–2709
- Xu X et al (2021) Deep learning-based tool wear prediction and its application for machining process using multi-scale feature fusion and channel attention mechanism. Measurement 177:109254
- Liao Y et al (2021) Manufacturing process monitoring using timefrequency representation and transfer learning of deep neural networks. J Manuf Process 68:231–248
- 34. Cheng M et al (2022) Prediction and evaluation of surface roughness with hybrid kernel extreme learning machine and monitored tool wear. J Manuf Process 84:1541–1556
- Goodfellow I, Bengio Y, Courville A (2016) Deep learning. MIT Press, USA
- Carbone N et al (2023) Assessment of milling condition by image processing of the produced surfaces. Int J Adv Manuf Technol 124(5):1681–1697
- Wu P et al (2022) A physics-informed machine learning model for surface roughness prediction in milling operations. Int J Adv Manuf Technol 123(11):4065–4076
- Cheng M et al (2021) Prediction of surface residual stress in end milling with Gaussian process regression. Measurement 178:109333
- Papananias M et al (2023) A probabilistic framework for product health monitoring in multistage manufacturing using Unsupervised Artificial Neural Networks and Gaussian Processes. Proc Inst Mech Eng Pt B J Eng Manuf 237(9):1295–1310
- Leco M, McLeay T, Kadirkamanathan V (2022) A two-step machining and active learning approach for right-first-time robotic countersinking through in-process error compensation and prediction of depth of cuts. Robot Comput Integrated Manuf 77:102345

- Tapia G, Elwany AH, Sang H (2016) Prediction of porosity in metal-based additive manufacturing using spatial Gaussian process models. Addit Manuf 12:282–290
- Wan J, McLoone S (2017) Gaussian process regression for virtual metrology-enabled run-to-run control in semiconductor manufacturing. IEEE Trans Semicond Manuf 31(1):12–21
- Rasmussen CE, Williams CK (2006) Gaussian processes for machine learning. MIT Press, USA
- Shi JQ, Choi T (2011) Gaussian process regression analysis for functional data. CRC Press, Boca Raton, FL
- Song G et al (2024) A multi-target predictive model for predicting tool wear and surface roughness. Expert Syst Appl 251:123779
- Qiang B et al (2023) Application of cutting power consumption in tool condition monitoring and wear prediction based on Gaussian process regression under variable cutting parameters. Int J Adv Manuf Technol 1241:37–50
- Zhao C, Lv J, Du S (2022) Geometrical deviation modeling and monitoring of 3D surface based on multi-output Gaussian process. Measurement 199:111569
- Papananias M et al (2022) A Bayesian information fusion approach for end product quality estimation using machine learning and on-machine probing. J Manuf Process 76:475

 –485
- JCGM 100:2008 Evaluation of measurement data guide to the expression of uncertainty in measurement, GUM 1995 with minor corrections. Joint Committee for Guides in Metrology
- JCGM 106:2012 Evaluation of measurement data the role of measurement uncertainty in conformity assessment. Joint Committee for Guides in Metrology
- 51. Migon HS, Gamerman D, Louzada F (2014) Statistical inference: an integrated approach, 2nd edn. CRC Press, Boca Raton, FL
- Quinonero-Candela J, Rasmussen CE (2005) A unifying view of sparse approximate Gaussian process regression. J Mach Learn Res 6:1939–1959
- Csató L, Opper M (2002) Sparse on-line Gaussian processes. Neural Comput 14(3):641–668
- Snelson E, Ghahramani Z (2005) Sparse Gaussian processes using pseudo-inputs. Proc Adv Neural Inf Process Syst 18, MIT Press
- Tresp V (2000) Mixtures of Gaussian processes. Proc Adv Neural Inf Process Syst 13, MIT Press
- Rasmussen C, Ghahramani Z (2001) Infinite mixtures of Gaussian process experts. Proc Adv Neural Inf Process Syst 14, MIT Press
- 57. Cohen S et al (2020) Healing products of Gaussian process experts. Int Conf on Mach Learn 37, PMLR 119
- 58. BS EN ISO 15530-3:2011. Geometrical product specifications (GPS). Coordinate measuring machines (CMM). Technique for determining the uncertainty of measurement. Use of calibrated workpieces or measurement standards. British Standard

Publisher's Note Springer Nature remains neutral with regard to jurisdictional claims in published maps and institutional affiliations.

